Published in final edited form as:
Proteins. 2009 August 15; 76(3): 731–746. doi:10.1002/prot.22385.

Order propensity of an intrinsically disordered protein, the cyclin-dependent-kinase inhibitor Sic1

Stefania Brocca[1,§], **Mária Šamalíková**[1,§], **Vladimir N. Uversky**[2,3], **Marina Lotti**[1], **Marco Vanoni**[1], **Lilia Alberghina**[1], and **Rita Grandori**[1,*]

[1]Department of Biotechnology and Biosciences, University of Milano-Bicocca, Piazza della Scienza 2, 20126 Milan, Italy

[2]Center for Computational Biology and Bioinformatics, Institute for Intrinsically Disordered Protein Research, Department of Biochemistry and Molecular Biology, Indiana University School of Medicine, Indianapolis

[3]Institute for Biological Instrumentation of the Russian Academy of Sciences, Pushchino 142290, Russia

Abstract

Intrinsically disordered proteins (IDPs) carry out important biological functions and offer an instructive model system for folding and binding studies. However, their structural characterization in the absence of interactors is hindered by their highly dynamic conformation. The cyclin-dependent-kinase inhibitor (Cki) Sic1 from *Saccharomyces cerevisiae* is a key regulator of the yeast cell cycle, which controls entrance into S phase and coordination between cell growth and proliferation. Its last 70 out of 284 residues display functional and structural homology to the inhibitory domain of mammalian p21 and p27. Sic1 has escaped systematic structural characterization until now. Here, complementary biophysical methods are applied to the study of conformational properties of pure Sic1 in solution. Based on sequence analysis, gel filtration, circular dichroism (CD), electrospray-ionization mass spectrometry (ESI-MS), and limited proteolysis, it can be concluded that the whole molecule exists in a highly disordered state and can, therefore, be classified as an IDP. However, the results of these experiments indicate, at the same time, that the protein displays some content in secondary and tertiary structure, having properties similar to those of molten globules or pre-molten globules. Proteolysis-hypersensitive sites cluster at the N-terminus and in the middle of the molecule, while the most structured region resides at the C-terminus, including part of the inhibitory domain and the casein-kinase-2 (CK2) phosphorylation target S201. The mutations S201A and S201E, which are known to affect Sic1 function, do not have significant effects on the conformational properties of the pure protein.

Keywords

Disorder prediction; protein-protein interactions; protein folding; molten globule; limited proteolysis; mass spectrometry; circular dichroism; protein phosphorylation; cell cycle; *Saccharomyces cerevisiae*

[*]Correspondence and requests of materials should be addressed to R.G. e-mail: rita.grandori@unimib.it Tel. +39 02 64483363, Fax. +39 02 64483565.
[§]S.B. and M.Š. contributed equally to the experimental work.

Introduction

Many naturally occurring proteins have been shown to lack rigid three-dimensional structure *in vitro*, existing instead as dynamic ensembles of inter-converting conformations. Many of these proteins acquire an ordered structure only upon binding to specific intracellular partners or by functional regulation *via* posttranslational modifications.1-9 In isolation, these proteins exhibit a highly dynamic structure that is resembling more the denatured rather than native state of "normal" globular proteins. Intrinsically disordered proteins (IDPs) have attracted a great deal of interest since it became clear that their lack of structural specificity is of physiological importance and does not simply result from improper handling *in vitro*. 10-12 Indeed, structural disorder characterizes a broad class of regulatory proteins, which all share the feature to bind multiple interactors.13-19 Intrinsic disorder is a common property of many protein types especially among the proteins involved in signal transduction and transcription regulation. Interest towards this feature is increasing also because structural disorder contributes to the gap between functions and structures in protein databases.

The dynamic properties of IDPs are considered to be instrumental to adaptation to different interaction surfaces and to favor rapid formation and dissociation of the complexes, as required for efficient intracellular regulatory networks.13 Thus, it seems that the flat energy landscape that governs conformational transitions of these proteins in solution is a selected feature for which their amino acidic sequences have been optimized, in order to keep the polypeptide chain in a sort of totipotent state that can then differentiate into distinct non-covalent complexes depending on the environmental conditions.20,21 Computational methods predict that IDPs are much more prevalent in domains from eukaryotic or viral proteins than in bacterial or archea proteins.22

The yeast protein Sic1 is a central regulatory protein of the yeast cell cycle, acting as inhibitor of the cyclin-dependent protein kinases by forming ternary complexes with kinases and their cognate cyclins.23 A well established role of Sic1 is to control the timing of entrance in S phase during the yeast cell cycle by inhibiting the complex Cdk1-Clb5/6, whose activity is required for the G1-to-S transition.24 The inhibition is released upon ubiquitin-dependent Sic1 degradation, which is, in turn, triggered by Sic1 phosphorylation at multiple sites in its N-terminal region.25,26 However, Sic1 is involved in several other intracellular processes such as exit from mitosis,27,28 coupling cell growth to cell cycle, 27-30 and signaling within the Tor31 and Hog32 stress-response pathways. As for other regulatory IDPs, the pleiotropic phenotype associated to Sic1 could be related to highly promiscuous interactions enabled by an intrinsically disordered structure.

Sic1 is a 284-amino acid protein with theoretical molecular mass 32,223 Da and isoelectric point 7.89. Its minimal fragment required for *in-vivo* inhibition of the Cdk1-Clb5/6 activity has been mapped to the last 70 amino acids.33 This C-terminal domain has been shown to be structurally and functionally homologous to the inhibitory domains of p21 and p27,34 mammalian tumor-suppressor proteins and well characterized members of the IDP class. 1,23,35,36 A crystallographic structure of the inhibitory domain of human p27 bound to the Cdk2-cyclin A complex has been reported.37 Although very poor sequence similarity links Sic1 to p21 and p27, molecular modeling of the Sic1 inhibitory domain could be performed based on the alignment of Sic1 predicted and p27 experimental secondary structure.34 The model docked onto the Cdk2-cyclin A complex displays a well formed interaction surface with proper contacts that should allow formation of a stable ternary complex. Such an interaction has also been shown experimentally,38 indicating evolutionary conservation of the key structural features for intermolecular recognition. On the basis of this evidence, Sic1 can be considered as a member of the IDP protein class, at least considering its C-terminal

domain. However, in spite of intensive studies on Sic1 function *in vivo*, no structural characterization or computational models on the full-length protein have been reported.

Another factor that could play a role modulating Sic1 conformational transitions, besides interactions with other proteins, is its posttranslational modification *via* phosphorylation. In particular, the recently detected phosphorylation on S201 by CK2, different from the phosphorylation events in the N-terminal region, does not seem to control Sic1 intracellular levels but, rather, to affect Sic1 affinity for intracellular partners.[27,28,38,39] Indeed it has been shown that a Sic1 peptide encompassing S201 binds more strongly to the mammalian Cdk2-cyclin A complex in its phosphorylated than in its non phosphorylated form.[38] Mutations of the residue S201 that either impair (S201A) or mimic (S201E) phosphorylation by CK2 alter the coordination between cell growth and cell-cycle progression in yeast cultures in exponential phase.[27] However, no data are available yet on the effects that this modification might have on the conformational properties of the protein.

Structural characterization of proteins in disordered conformation is technically difficult, but it is important to better understand folding transitions to ordered states. Increasing evidence indicates that residual structure characterizes globular proteins under various denaturing conditions,[40] as well as various IDPs in the absence of binding partners.[15] A promising approach to this technically challenging problem is offered by a multiparametric analysis, which employs a set of complementary biophysical methods sensitive to distinct structural features.[41] In this study, such an approach is applied to the investigation of Sic1 structural properties and conformational transitions *in vitro* by the use of bioinformatics, gel filtration, CD, ESI-MS, and limited proteolysis. The results show that Sic1 is a highly disordered protein, nevertheless endowed of a partially collapsed structure. The most structured region maps at the C-terminus, partially overlapping to the inhibitory domain.

Materials and methods

Disorder predictions

Disorder predictions for the Cki Sic1 were performed by *PONDR®VLXT*,[42] *PONDR®VSL2*,[43] *PONDR®VL3*,[42,44] *IUPred*[45] and *RONN*.[46] *PONDR®* (Predictors of Natural Disordered Regions) is a neural network based on local amino acid composition, flexibility and hydropathy. It is the merger of three predictors, one trained on *V*ariously characterized *L*ong disordered regions and two trained on *X*-ray characterized *T*erminal disordered regions.[7,44,47]

*PONDR®*VL3 predictor is a feed forward neural network that was trained on 152 *L*ong disordered regions characterized by *V*arious methods.[43, 48] This is one of the most accurate predictors of long disordered regions. The most recent advance in the *PONDR®* collection are the *VSL* predictors (trained on *V*ariously-characterized, *S*hort and *L*ong disordered regions), based on compositional differences of short and long disordered regions. *PONDR®VSL2*, which uses support vector machines (SVMs), has achieved high accuracy and improved performance on short disordered regions, while maintaining high performance on long disordered regions.[49]

IUPred is an algorithm that evaluates intrinsic disorder based on the energy resulting from inter-residue interactions.[21] This predictor is based on the observation that, while the structure of ordered proteins is stabilized by a large number of inter-residue interactions, intrinsically disordered proteins do not have sufficient inter-residue interactions.[45,50] Finally, *RONN* was designed to predict disordered structures based on functional alignments.[46]

The output of these predictors is a position-dependent score for disorder propensity, which varies between 0 and 1. A threshold of 0.5 for prediction of structural disorder is generally applied.51 Cumulative distribution functions (CDF) were generated using *PONDR®VLXT* output scores as described by Oldfield and coworkers.3 Charge-hydropathy (CH) plots were generated as described by Uversky and coworkers.3,51 Ordered and disordered proteins plotted in the CH-space were shown to be separated by a linear boundary, with disordered proteins above the boundary and ordered proteins below.3 This boundary is described by the following relationship,7

$$\langle H\rangle \leq \langle H\rangle_b = \frac{\langle R\rangle + 1.151}{2.785}$$

where <H> and <R> are the mean hydropathy and the mean net charge of the given protein, respectively, whereas $\langle H\rangle_b$ is the "boundary" mean hydropathy value, below which a polypeptide chain with a given <*R*> will be most probably unfolded. The mean hydropathy, <*H*>, is defined as the sum of the normalized hydrophobicities of all residues divided by the number of residues in the polypeptide. The mean net charge, <*R*>, is defined as the net charge at pH 7.0, divided by the total number of residues. CH-plot and CDF analyses were performed using software developed at Molecular Kinetics Inc. and accessible at http://www.PONDR.com.

α-MoRF predictions

The predictor for α-helix-forming *M*olecular *R*ecognition *F*eature (α-*MoRF*) is based on the observation that predictions of order in otherwise highly disordered proteins correspond to protein regions that mediate interaction with other proteins or DNA. This predictor focuses on short (~20 residues) binding sites within long regions of disorder that are likely to form helical structure upon binding.6,52 It follows a stacked architecture, with a first level where *PONDR®VLXT* is used to identify sequences with helical propensity and then a second level to evaluate the likelihood for such sequences to constitute binding sites based on attributes of the sequence itself and the surroundings.

Compositional profiling

The amino acid composition of Sic1 and that of a set of disordered proteins was compared with a set of ordered proteins.53 The fractional difference in composition between Sic1 (or a set of disordered proteins) and a set of ordered proteins was calculated for each amino acid as $(C_X\text{-}C_{order})/C_{order}$, where C_X is the content in a given amino acid of Sic1 (or a set of intrinsically disordered proteins for the *DisProt* database54) and C_{order} is the corresponding value in a set of ordered proteins.

Solvents

Acetonitrile G *CHROMASOLV* for HPLC (super gradient grade), ammonium hydrogen carbonate, ammonium acetate (7.5 M solution), and 2,2,2-trifluoro ethanol (TFE) were of highest purity and were purchased from Sigma (Sigma Aldrich, St. Louis, MO, USA).

Recombinant DNA techniques

The *Escherichia coli* DH5α strain has been used for cloning and BL21 Rosetta (Novagen, EMD Chemicals Inc., Darmstadt, D) for protein expression. Standard recombinant DNA manipulations were performed according to Sambrook.54 The entire open reading frame of the *SIC1* gene has been cloned by excision from the plasmid pIVEX2.4a-*SIC1*55 and subsequently modified at its 5' and 3' terminus by *back-to-back* PCR55 to adapt its sequence to functional expression in pET21a vector and to add a C-terminal His_6 tag. Thus the 855 bp

*Bam*HI-*Bam*HI fragment from pIVEX2.4a-*SIC1* was cloned into the *Bam*HI restriction site of the pET21a vector and the DNA was inserted into *E. coli* DH5α cells, resulting in clone pET21[^{T7tag} SIC1]. Site-directed mutagenesis was performed employing the TripleMaster® PCR System (Eppendorf) on the entire pET21[^{T7tag} SIC1]. The DNA *Bam*HI-*Bam*HI insert was first modified to fuse in frame the C-terminus of Sic1 and the esahistidine tag. The oligonucleotides were: 5'-ACG TTG GCC ATG CTC TTG ATC CCT AGA T-3', 5'-ACG TTG GCC ACC ACC ACC ACC ACC ACC-3'. These primers result in the deletion of the downstream *Bam*HI site and part of the pET21 multiple cloning site, while introducing a recognition site for *Msc*I (shaded) The resulting clone is pET21[^{T7tag} SIC1^{HIS6}], which was further modified to delete the T7 tag sequence (coming from the pIVEX vector) fusing in frame the *SIC1* sequence and the promoter. The oligonucleotides were: 5'-ACT CCG TCG ACC CCA CCA AGG TCC-3', 5'-ACG TGT CGA CGG AGT CAT ATG TAT ATC TCC TTC-3'. These primers result in the deletion of the upstream *Bam*HI site and introduce a recognition site for *Sal*I (shaded). The resulting clone is pET21[SIC1^{HIS6}].

Sic1 site-directed mutagenesis on Ser201 to alanine (S201A) or glutamic acid (S201E) was performed by *back-to-back* PCR on the entire pET21[SIC1^{HIS6}]. The oligonucleotides used for mutagenesis were: 5'-CCA G<u>AT C</u>TC AAG **A**AG AGG AAG ACG AGG AAG-3', 5'-GTC TTC C**G**C TTC TTG AGA TCT GGC GTC ATT TTT CG -3' for S201E; and 5'-CCA G<u>AT C</u>TC AAG **C**AG AGG AAG ACG AGG AAG-3', 5'-GTC TTC C**T**C TTC TTG AGA TCT GGC GTC ATT TTT CG -3' for S201A. The primers provide a single base mismatch (bold) to mutate the amino acid 201 and a triplet mismatch (underlined) to generate, without altering the translation code, a *Bgl*II restriction site (shaded) not present in the wild type sequence and used to generate sticky-end PCR products to be self-ligated for circularization by the T4 DNA ligase.56 The correct identity of the resulting recombinant plasmids pET21[SIC1^{HIS6}S201A] and pET21[SIC1^{HIS6}S201E] was checked by DNA sequencing on both strands.

Expression and purification of Sic1-His$_6$

Transformed *E. coli* cells BL21-Rosetta were cultured in 1L low-salt Luria-Bertani broth containing 100 mg/L ampicillin and 34 mg/L chloramphenicol at 37°C until OD_{600} ~0.5, and induced for 2 h, unless otherwise stated, by 200 μM isopropyl thio-β-D-galactoside (IPTG) at 30 °C. *E. coli* cells expressing recombinant Sic1-His$_6$ were harvested by centrifugation and resuspended in 1/200 volume of lysis buffer, 50 mM Na_2HPO_4, pH 8.0, 10 mM imidazole, 300 mM NaCl, containing protease inhibitors cocktail for use in purification of histidine-tagged proteins (Sigma Aldrich, St. Louis, MO, USA). Cells were then either directly extracted or stored at -20 °C. Protein extraction and heat treatment were carried out at once by incubating cells suspension at 99 °C for 10 min. The crude extracts were then cooled 10 min on ice and centrifuged 10 min at 10000 rpm to separate cellular debris and insoluble proteins. Recombinant Sic1, recovered as soluble protein, was further purified from the supernatant by immobilized-metal affinity chromatography (IMAC) on Ni^{2+}/NTA beads as described (Qia expressionist Handbook, Qiagen) and eluted in 50 mM Na_2HPO_4, pH, 8.0, 250 mM imidazole, 300 mM NaCl.

In order to evaluate the effects of heat treatment on the protein conformation, an alternative protocol has been developed. Cells were lysated by sonication by eight 15-s pulses on a Fisher sonicator model 300, relative output 50%, on ice. Sic1 was purified from the soluble fraction by sequential metal-affinity, desalting (*PD-10*, General Electric-Amersham Biosciences, Uppsala, Sweden), and cation-exchange (*CM-Sephadex* General Electric-Amersham Biosciences, Uppsala, Sweden) chromatography. Sic1 is eluted from the CM column by 50 mM Na_2HPO_4, pH 6.2, 600 mM NaCl. Such preparations were used to test the effect of heat treatment by CD and ESI-MS. The purified protein from either protocol was finally obtained in the desired buffer by either gel filtration on *PD-10* columns or

several cycles of dilution and ultrafiltration on *Vivaspin 500* centrifuge units (cutoff 5,000 Da, Sartorius Biolab, D).

The final Sic1 preparations were of at least 95% purity, as judged by desitometric analysis of SDS-PAGE gels. Protein concentration was determined by absorbance at 280 nm on a *Nanodrop* spectrophotometer (Nanodrop Technologies, Inc.,Wilmington, DE, USA) using the calculated molar extinction coefficient of 8,480 M^{-1} cm^{-1}. SDS-PAGE were carried out by the Laemmli protocol57 on 12% (for intact protein analysis) or 16% (for proteolysis experiments) acrylamide gels, subsequently stained by *GelCode Blue* (Pierce, Illinois, IL, USA). Western blots onto nitrocellulose filters (Schleicher and Schuell BioScience, Inc., Keene, NH, USA) were decorated by purified anti-Sic1 polyclonal antibodies28 or anti-His_6 polyclonal antibodies (Santa Cruz Biotechnology, Inc.) at 1:1,000 dilution. An enhanced chemiluminescence system (*ECL* Western Blotting Substrates, Pierce, IL, USA) was used for antibodies detection.

Analytical gel filtration

Gel filtration was performed on an *ÄKTApurifier* liquid-chromatography system (General Electric-Amersham Biosciences, Uppsala, Sweden), using a prepacked, 30×1 cm *SuperdexTM 75 HR* column (General Electric Life Science, GE Co., USA). Chromatography was carried out at room temperature in 50 mM Na_2HPO_4, pH 8.0, 200 mM NaCl at a flow rate of 0.5 ml/min and monitored by absorbance at 280 nm. Calibration was performed using the following standards (2 mg/ml): horse cytochrome *c* (12,400 Da), horse myoglobin (17,600 Da), chicken ovalbumin (45,000 Da), and bovine serum albumin (66,400 Da) (Sigma Aldrich, St. Louis, MO, USA).

Limited proteolysis

Trypsin (Promega Corporation, Madison, WI, USA) and chymotrypsin (Sigma Aldrich, St. Louis, MO, USA) stock solutions were prepared by dissolving the commercial powders in 1 mM HCl at a final concentration of 1 mg/ml and stored at -80 °C. Reactions were carried out at room temperature in 50 mM ammonium acetate, pH 6.5, 100 mM NaCl. Aliquots were removed over a time course and the reaction was stopped by the addition of SDS-PAGE loading buffer and immediate boiling for 3 min.

In-gel digestion

Bands of interest were excised from the polyacrylamide gels, cut into small pieces and destained by repeated washing cycles alternating 50 mM ammonium hydrogen carbonate and pure acetonitrile. After complete destaining, gel particles were dehydrated by acetonitrile, covered with a trypsin solution (12.5 ng/ml in 50 mM ammonium hydrogen carbonate, pH 8.0) and incubated 1 h on ice. The excess of liquid was removed, gel pieces were covered with a solution of 50 mM ammonium hydrogen carbonate, pH 8.0 and incubated overnight at 37 °C. Tryptic peptides were extracted from gel particles by repeated cycles of alternating incubations in pure acetonitrile and 1% formic acid. Samples were lyophilised, resuspended in 1% formic acid, and desalted by *ZipTip* (Millipore, Carrigtwohill, Ireland) before ESI-MS analysis.

Circular dichroism

CD spectra were recorded on a spectropolarimeter *J-815* (JASCO corporation, Japan), equipped with a Peltier thermoregulation system, in a 1-mm pathlength cuvette. Reported spectra are acquired with data pitch 0.5 nm, averaged over three acquisitions, and smoothed using the Savitzky-Golay algorithm.58 Deconvolution of CD spectra were performed by the *CDPro* software package58 using the reference protein set *SDP448*, containing both native

and denatured proteins. The reported percent values of secondary-structure content are averaged over the results of three different algorithms: *SELCON3*, *CDSSTR* and *CONTIN*.59 Spectra at variable temperature were acquired with the same parameters as above, and temperature steps of 20 °C and scanning velocity 20 nm/min. Measurements at fixed wavelength were performed with data pitch 0.2 °C and temperature slope 1 °C/min. The buffer solutions without the protein were used as blank.

Mass spectrometry

ESI-MS experiments were performed on a hybrid Quadrupole-Time-of-Flight (q-TOF) mass spectrometer (*QSTAR ELITE*, Applied Biosystems, Foster City, CA, USA) equipped with a nano-electrospray ionisation sample source. Metal-coated borosilicate capillaries (Proxeon, Denmark) with medium-length emitter tip of 1-μm internal diameter. The instrument was calibrated with a standard solution containing cesium iodide (Cs+ 132.9 Da) and the synthetic peptide ALILTLVS (MH+ 829.5 Da, Applied Biosystems, Foster City, CA, USA). Peptide identification was performed using the *MASCOT* software with following parameters: 2 missed cleavages, peptide tolerance 0.6 Da, MS/MS tolerance 0.4 Da, peptide charges 2+ and 3+. Only monoisotopic masses were considered as precursor ions.

Spectra of intact Sic1 were acquired in the 500-2,000 *m*/*z* range, with accumulation time 1 sec, ion-spray voltage 1,200-1,400 V, declustering potential 60-80 V, and instrument interface at room temperature. Spectra were averaged over a time period of 2 min. Spectra of Sic1 tryptic peptides were acquired in the 400-1,500 *m*/*z* range, with accumulation time 1.5 s, ion-spray voltage 1,200 V, declustering potential 80 V, with active „information dependent acquisition“ (IDA), using rolling collision energy to fragment peptides for MS/MS analysis. Liquid chromatography coupled to MS analysis was performed on a nano-HPLC instrument (*Tempo*, Applied Biosystems, Foster City, CA, USA) using a *VYDAC MS* C18 column, 0.075×150mm, 5 μM particle size, 300 Å pore size (Alltech, Springfield, KY, USA) at a flow rate of 250 nL/min, equilibrated in 0.1% formic acid, and developed by a linear gradient 0-60% acetonitrile in 1% formic acid.

Results

Sequence analysis

Figures 1 and 2 summarize Sic1 structural features predicted by sequence analysis. Figure 1 reports predicted conformational properties of this protein. The consensus secondary-structure prediction derived from several different algorithms hints to the existence of large portions in random-coil conformation, particularly within the N-terminal half of the molecule (*Jnet* line). The prediction also includes extended segments with a predominance of α-helices and with a higher content in regular secondary structure within the C-terminal moiety. Prediction of solvent accessibility60 indicates that very few positions have strong burial propensity, and also these are clustered in the C-terminal half of the molecule (*SUBacc* line). The *GLOBE* algorithm42 predicts a non-globular structure for the entire protein (data not shown), based on a large difference between the number of predicted exposed residues (226) and the number of expected exposed residues (120).

Disorder prediction by several different algorithms indicates a high degree of intrinsic disorder in Sic1 (Figure 2A). The disorder profiles for all the predictors employed, as well as the curve corresponding to the consensus score distribution, are mostly located above the generally applied threshold of 0.5,51 clearly showing that Sic1 is a highly disordered protein, with particularly high disorder propensity in the N-terminal region. The output of the *PONDR®VLXT* predictor has been used to generate a CDF curve (Figure 2B). CDF analysis summarizes the per-residue disorder predictions by plotting *PONDR* scores against

their cumulative frequency within the protein sequence. The ordinate of each point of the graph gives the proportion of residues with a *PONDR* score less or equal to the abscissa. This analysis is based on a binary disorder classifier which predicts whole proteins as either mostly disordered or mostly ordered, based on whether a CDF curve is above or below a reference boundary curve.3 Figure 2B shows that the Sic1 curve lies below the boundary, confirming that Sic1 is a mostly disordered protein.

This conclusion is consistent with the results of the Sic analysis by another binary disorder classifier, the CH signature. Simultaneous observation of low mean hydropathy (<*H*>) and high mean net charge (<*R*>) is typical of IDPs.3 Analysis of the Sic1 amino acid sequence shows that this protein is characterized by <*H*> = 0.3834, <*R*> = 0.0035, and $<H>_b$ = 0.4145, thus fulfilling the requirement for the natively unfolded proteins, namely that <*H*> < $<H>_b$ (0.3834 < 0.4145).51 Thus, evaluation of conformational properties by disorder predictors, CDF analysis and CH-plots suggests a mostly disordered structure for the whole Sic1 molecule. This is generally taken as evidence that the protein belongs to the class of native coils or native pre-molten globules.7 However, the spot corresponding to Sic1 lies in the close proximity of the boundary in the CH-plot (not shown), indicating that this protein might have partially collapsed structure.

Figure 2C compares the results of the Sic1 compositional profiling 52 with that of the intrinsically disordered proteins from the *DisProt* database.53 Residues that are less abundant in Sic1 (or in a set of disorder proteins) than in typical ordered proteins are shown by negative bars ($C_X<C_{order}$) and those that are enriched are shown by positive bars ($C_X>C_{order}$). Compositional profiling of Sic1 reveals that in comparison with typical ordered proteins, Sic1 is noticeably depleted in order-promoting residues, including W, Y, C, I, L, V, M, and H, and is highly enriched in disorderpromoting residues, such as T, R, Q, S, N, P, E, and K (Figure 2C).

The Sic1 sequence has also been analyzed by α-*MoRF*, a predictive tool specifically developed to reveal short interaction-prone segments in disordered proteins that could undergo a coil-to-helix transition induced by intermolecular contacts.34 This algorithm identifies potential binding sites in three putative α-helical intermolecular recognition features: residues 75-93, 142-160, and 240-258 (Figure 1). Altogether, these results suggest that the whole Sic1 protein is mainly disordered, with an intrinsic propensity for ordered structure (Figure 1).41›61

Protein expression and purification

The recombinant protein Sic1-His_6 was expressed in BL21-Rosetta *E. coli* cells. Maximal accumulation of the intact product is seen after 2-h induction by IPTG at 30 °C. The protein is purified essentially in two steps involving heat treatment and IMAC (Figure 3). It was reasoned that an intrinsically disordered protein might be enriched in the soluble fraction of heat-treated crude extracts since no global unfolding and, therefore, no big changes in aggregation propensity are expected to take place in response to the treatment. Indeed, preparation of crude extracts by incubation at 99 °C for 10 min, followed by removal of insoluble material, results in substantial purification of Sic1, as shown by the gel in Figure 3. The effects of heat on the protein conformation are fully reversible, as indicated by CD and ESI-MS analysis on Sic1 purified by an alternative protocol that does not involve heat treatment (see *Materials and methods*). The spectra of such protein preparations before and after heat treatment are identical (data not shown).

As typical of IDPs, Sic1 turns out to be prone to proteolytic attack (Figure 3). Its partial degradation is not completely prevented even by the presence of protease inhibitors throughout the purification procedure. Degradation is enhanced by increasing duration or

temperature of IPTG induction, as well as by sample aging or scaling up of the purification procedure. The protein also tends to aggregate in pure water (data not shown). Another feature that Sic1 shares with other IDPs is an anomalous migration on SDS-PAGE. Indeed, the apparent molecular weight derived from SDS-PAGE is ~37 kDa, higher than the isotopically averaged value calculated for Sic1-His_6 based on the amino acid sequence (33,046 Da) and measured by mass spectrometry (33,050 +/- 2 Da). Such a behavior could result from poor interaction with SDS due to the anomalous amino acid composition of IDPs,[3,44] in particular a lower content in hydrophobic residues and a higher content of charged residues than average.[62-64]

Conformational properties of pure Sic1

In order to get a first experimental indication about Sic1 conformational properties, the hydrodynamic behavior of the purified protein has been investigated by gel-filtration chromatography in 50 mM sodium phosphate, pH 8.0, 200 mM NaCl. Protein standards with known globular structure were used for calibration in the molecular-weight range 12.4-66.4 kDa and, thus, bracketing Sic1 molecular weight. As can be seen in Figure 4, the expected logarithmic relationship between mass and elution time is observed for the standards. Under these conditions, Sic1 elutes as a single symmetric peak between ovalbumin and bovin serum albumin. Its apparent molecular weight is ~50 kDa, ~50% higher than the real one. Thus, Sic1 in solution has a much larger hydrodynamic radius than expected for a protein of its size in a compact, globular conformation, indicating that the protein structure is, at least partially, disordered. In particular, these results indicate an increase of ~1.5-fold in the hydrodynamic volume of the protein, relative to its hypothetical compact, globular structure. Such a degree of compactness has been ascribed to proteins in their molten-globule state.[65]

Sic1 conformational properties have been further investigated by far-UV CD and ESI-MS analysis, which offer complementary information on protein secondary and tertiary structure, respectively. These techniques have different buffer requirements, since volatility is needed for ESI-MS and high transparency for CD measurements down to 190 nm. Thus same ionic strength and pH have been maintained for both kinds of experiment by using 50 mM ammonium acetate, pH 6.5 as MS-ESI buffer and 50 mM sodium phosphate, pH 6.5 as CD buffer.

The far-UV CD spectrum of Sic1 (Figure 5) is characterized by a shoulder at 222 nm and an intense negative minimum at ~202 nm. These features indicate that Sic1 in solution is mostly disordered but contains some helical structure (~9%), in agreement with the predictions reported in Figure 1. No significant spectral changes are observed varying NaCl concentration between 0 and 300 mM (Figure 5, upper inset). Also mutations in position 201 do not have significant effects on the secondary structure content, as indicated by the CD spectra of the mutants S201A and S201E compared to the wild-type protein (Figure 5, lower inset). Thus, the effects of these mutations that have been described *in vivo* and *in vitro* can not be simply interpreted in terms of different conformational properties of the protein itself. CD measurements down to 200 nm in 50 mM ammonium acetate, pH 6.5 (ESI buffer) gave very similar results to those reported in Figure 5 (data not shown).

Nano-electrospray is a mild ionization technique, which is known to preserve non-covalent interactions responsible for protein conformation and supramolecular complexes.[66-70] In addition, charge-state distributions (CSDs) obtained by ESI-MS have been shown to be sensitive to the compactness of protein tertiary structure[71] while quite insensitive to secondary-structure content.[72,73] Thus, ESI-MS offers a global probe for protein conformational analysis which is nicely complementary to CD data, and has also been already applied to conformational analysis of IDPs.[74] The ESI-MS spectrum of intact Sic1 in 50 mM ammonium acetate, pH 6.5, shows a single, broad CSD centered on the 28+ ion

(Figure 6A). The CSD of the protein under denaturing conditions such as 1% formic acid (Figure 6B) is bimodal (maxima at 26+ and 39+), indicating coexistence of two distinct conformational states. The further addition of 50% acetonitrile reduces the component centered on the 26+ ion and results in a minor shift of the highly charged component to 43+ (Figure 6C). We assign the latter to the fully unfolded protein and the component centered on the 26+/28+ ion to a partially folded form of the protein. Indeed, a completely folded globular structure for a protein of this size is predicted to result in an average charge state of 14+.75 Thus, Sic1 can be brought to a more extended conformation by the addition of denaturing agents, indicating that the protein in ammonium acetate contains some degree of tertiary structure. Together with the CD data reported above, these results suggest that pure Sic1 in solution populates a molten-globule-like state.

Folding induced by TFE

Disordered regions of IDPs are characterized by an intrinsic propensity to form ordered secondary structure, which can be enhanced by the addition of TFE, a compound known to stabilize protein secondary structure by promoting the burial of polypeptide backbone groups.76 Conformational transitions induced by TFE in other IDPs take place at relatively low concentrations of the co-solvent (10-30%).4,65 Figure 7 illustrates the effect of increasing TFE concentrations on the far-UV CD spectrum of Sic1 wild-type and S201A, S201E mutants. The results reveal a pre-transition baseline in the TFE effect up to a concentration of ~20% and a highly cooperative coil-to-helix transition above 20% TFE, characterized by an isodichroic point around 200 nm. The transition slowly tends to a plateau above 50% TFE. The spectra at 50% TFE and above are typical of a highly helical structure, with well formed negative minima at 222 and 208 nm and a positive maximum at 190 nm. Deconvolution results give ~40% helical structure for the protein at 65% TFE. The protein tends to precipitate at TFE concentrations above 65%. As shown in the figure inset, the TFE response of the S201A and S201E mutants is very similar to that of the wild-type protein.

Folding induced by heat

Mesophilic IDPs also have a peculiar response to heat, frequently showing folding induced by heating above room temperature.77,78 Figure 8 shows the heat dependence of Sic1 far-UV CD, indicating a progressive increase in helix content going from 20 to 80 °C. The spectra display an isodichroic point indicative of a two-state transition. The effect is modest and the spectrum reverts to the initial features after re-cooling at room temperature (inset Figure 8).

Limited proteolysis

The action of proteases is affected by the accessibility and flexibility of the substrate polypeptide chain, making disordered regions an easy target for proteolytic attack.79-83 Indeed, it has been established that sites most prone to proteolysis in folded proteins are typically found at flexible and exposed loops83,84, and are typically absent in ordered regions rich in regular secondary structure.41,85-88 That is why, at low enough enzyme-to-substrate ratios, it is possible to discriminate among putative cleavage sites based on their susceptibility to proteolysis, gaining insights on the structure and dynamics of distinct regions of the protein structure. Limited proteolysis has been used for identification and characterization of IDPs.78

This technique has been employed here to map hypersensitive sites and resistant fragments of Sic1, which would correspond, respectively, to the most disordered and the most structured regions of the molecule in solution. It is generally advisable to compare results obtained by proteases of different specificity, in order to discern structure effects from

sequence effects.65 Thus, even the spontaneous degradation taking place during the purification procedure can add useful information to deliberate proteolysis experiments carried out by the addition of specific proteases. Relevant to this regard is that spontaneous degradation gives rise to a very reproducible pattern of bands.

Five major bands (*a*-*e*) tend to accumulate below the band of intact Sic1, as detectable on Coomassie-stained gels (Figure 9). These fragments were first characterized by western blot. All of them are recognized by anti-Sic1 polyclonal antibodies, supporting their identification as Sic1 degradation fragments (data not shown). The three larger ones are also recognized by anti-His_6 antibodies (Figure 9) and, thus, contain an intact C-terminus. This result indicates that bands *a*-*c* are produced by progressive chopping from the N-terminus providing a first indication of particular instability of the N-terminal region of this protein. Bands *d* and *e* were in-gel digested by trypsin, and the resulting peptides were analysed by liquid chromatography coupled to tandem mass spectrometry (LC-MS/MS). The Sic1 peptides that could be identified in each band are shown in Figure 9. Band *d* contains fragments from both the N- and C-terminal moieties and, therefore, seems to derive from cleavage events approximately in the middle of the molecule combined to N-and C-terminal trimming. Band *e* contains fragments from the C-terminal region 178-260 (178-185, 194-233 and 236-260). Since the Sic1 sequence following residue 260 is extremely rich in basic residues, it is expectable that tryptic digestion products from this region are lost. Therefore, it is likely that band *e* extends beyond fragment 178-260 on the C-terminal side. On the other hand, the Sic1 sequence preceding residue 178 (PGTPS) corresponds to a peak in the predicted disorder profile (Figure 2A) and it is expected to be a good proteolysis target. Thus, the smallest fragment out of the five major degradation products seems to correspond approximately to the C-terminal half of the molecule, trimmed at both ends.

Figure 10 shows the time course of Sic1 degradation under conditions optimized to monitor proteolysis by trypsin (Panel A) and chymotrypsin (Panel B). Consistent with a mostly disordered protein structure, it was necessary to use quite low enzyme-to-substrate ratios (1:2,000-1:5,000), in order to detect intermediates of the degradation process. The starting samples contain already some degradation products, reflecting some unavoidable variability among protein preparations and difficult control of spontaneous degradation through scaled-up protein purification. The degradation patterns obtained with the two proteases are similar to each other and to those produced by spontaneous degradation in crude extracts. It is possible to detect accumulation of early fragments around 30 kDa, intermediate fragments around 16 kDa, and late fragments around 6 kDa. The latter persist after prolonged incubation times (> 20 min), when all the fragments at higher molecular weight have already disappeared. These results indicate that there are major differences in the susceptibility of cleavage sites within the Sic1 molecule and that some regions of the protein are more protected than others. The similar patterns observed with proteases of different specificity suggest that protection is caused by local protein conformation and not directly by sequence features.

The late fragments (bands *f* from trypsin and band *g* from chymotrypsin digestion) have been processed by tryptic in-gel digestion and the resulting peptides were analyzed by MS/MS. The results are reported in Figure 10. All the peptides identified from these bands derive from the C-terminal region of Sic1. These peptides span the region 178-233 in the case of trypsin and 198-233 in the case of chymotrypsin, and still contain numerous potential target sites for both proteases. Altogether the results from spontaneous and deliberate digestion indicate that proteolysishypersensitive sites cluster at the N-terminus and in the middle of the molecule, consistent with the disorder prediction reported above. The C-terminal region, at least from position 198 to 233, seems to be the most structured part of the Sic1 molecule in the absence of interactors.

Discussion

This work reports the first structural characterization of full-length Sic1, a central regulator of the yeast cell cycle. The first conclusion of this work is that Sic1 is an intrinsically disordered protein. Such a conclusion emerges from a consensus of bioinformatic predictions and experimental data, supporting its identification as a new member of the IDP class. Our results are in agreement with a recent NMR report on the isolated N-terminal 90 residues of the protein, which was published during revision of the present paper.89 In that work, chemical shift dispersion and nuclear Overhauser effect indicate a highly disordered structure of the Sic1 N-terminal fragment.

The second important conclusion of this work is that the disordered state of Sic1 in the absence of interactors is characterized by the presence of some intrinsic tertiary and secondary structure that makes it clearly different from a completely unfolded protein. The protein displays global compactness intermediate between that of a fully unfolded and a folded globular protein and can be ”denatured” by acids and organic solvents to a fully unfolded state. Thus, the properties of Sic1 in solution are reminiscent of those of molten globules or pre-molten globules.76،90 The isolated N-terminal fragment, too, displays some structural compactness and transient secondary and tertiary structure.89

As observed for many other IDPs, Sic1 undergoes coil-to-helix transitions induced by TFE and heat. The pronounced response of IDPs to TFE addition seems to reflect their potential to form ordered secondary structure,1 while the response to heat could be due to predominance of electrostatic interactions in the folding transitions of these proteins with peculiar charge-hydrophobicity features.91 More structural investigation will be needed to relate these transitions to the physiologically relevant conformational changes of Sic1.

This work focuses further on the localization of intrinsically structured regions within the Sic1 molecule. The the most structured moiety of the Sic1 molecule is located near the C-terminus, while the N-terminus turns out to be the most disordered region. Structured regions or subdomains have been characterized in other IDPs, such as stathmin/OP18,92 GCN4,23،36،93 and the Sic1-related p21 and p27.1،94 The intrinsic structure of IDPs could play a role counteracting protein degradation *in vivo* and offering locally structured regions that may serve as nuclei for the formation of interaction surfaces. This has been shown to be the case in the sequential mechanism of cyclin/kinase complex recognition by the inhibitory domain of p27.36،95 Consistently, the Sic1 proteolysis-resistant fragment identified in this work (178-233) overlaps with its inhibitory domain (215-284).

Thus, although Sic1, p21 and p27 are related disordered proteins, the domain that they have in common is the least disordered part of the protein. Also in p21 and p27, the inhibitory domain is the most structured region.96 However, no homology outside such domain links these proteins to Sic1. This fact could reflect relatively constant kinds of interactions involving the inhibitory domain, which might be “specialized” for binding at kinase active sites and to cognate cyclins,97 rather than adaptable to a variety of different interactors. Furthermore, the target kinases and cyclins, too, are evolutionary conserved, thus imposing similar selective pressure on the inhibitory domains.

The proteolysis-resistant C-terminal fragment of Sic1 also includes residue S201, the CK2 phosphorylation target. Sic1 phosphorylation at this site has been shown to affect the G1-to-S transition and the coordination between cell size and cell cycle *in vivo*, as well as to increase Sic1 affinity for the cyclin-kinase complex *in vitro*. More detailed structural information is needed in order to interpret the effect of phosphorylation at this site on the interaction with the cyclin-kinase complex. However, the results on the mutant proteins S201E and S201A reported here do not reveal appreciable effects of these substitutions on

Sic1 conformation in the unbound state, as observed instead in other instances, like p2798 and a calmodulin-derived peptide.1,99

The remarkable disorder of the Sic1 N-terminal region is likely related to the high density of phosphorylation sites, as suggested by the correlation observed for several other regulatory proteins.100 Multiple Sic1 phosphorylation within this intrinsically disordered region mediates dynamic complex formation with the ubiquitin ligase Cdc4.89,101 The highly disordered regions of Sic1 could also mediate promiscuous interactions. Continuously growing evidence of multiple intracellular functions of Sic1 actually hints to the possibility that its molecular partners might be a large number, as also indicated by the recent *in-vivo* mapping of the yeast interactome.102

It should also be underscored that some degree of disorder can persist in IDPs even within supramolecular complexes.102 Such “fuzziness” in protein-protein interactions could be beneficial, conferring adaptability, versatility and reversibility to the binding reaction.51 Thus, it is also possible that Sic1 regions with highest disorder propensity remain locally unstructured in the bound state, thus increasing the entropy of the bound state relative to a more typical ordered complex and contributing favorably to binding.89,103 This work offers a contribution to the characterization of Sic1 in its unbound state, which is needed to interpret transitions in the presence of interactors.

Conclusion

By describing the structural properties and the conformational transitions of Sic1 in the absence of interactors, this work sets the bases for the interpretation of molecular-recognition properties of this IDP. Our findings highlight structural features shared by mammalian and yeast Ckis. A conservation of order/disorder features emerges, although with inverted module sequences, beyond the relationship inferable by sequence similarity. This structural conservation likely reflects conserved interaction networks, which might be revealed by future work on Ckis complexes with intracellular partners.

Supplementary Material

Refer to Web version on PubMed Central for supplementary material.

Acknowledgments

We thank Paola Coccetti for providing the pIVEX[sic1] plasmid, and Vera Codazzi for technical assistance. We thank Luigi Casella for helpful discussions and critical comments on the manuscript. This work was supported by grants MIUR-Italbionet to L.A., Miur Cofin 2006 to MV, 12-1-181 and 12-1-209 from the University Milano-Bicocca (“Fondo Ateneo per la Ricerca”) to R.G., R01 LM007688-01A1 to V.N.U. and GM071714-01A2 from the National Institutes of Health and by the Program of the Russian Academy of Sciences for the "Molecular and cellular biology" to V.N.U. We gratefully acknowledge the support of the IUPUI Signature Centers Initiative. M.Š. is recipient of a postdoctoral fellowship “Assegno di Ricerca” of the University Milano-Bicocca.

References

1. Galea CA, Wang Y, Sivakolundu SG, Kriwacki RW. Regulation of cell division by intrinsically unstructured proteins: intrinsic flexibility, modularity, and signaling conduits. Biochemistry. 2008; 47:7598–7609. [PubMed: 18627125]
2. Fink AL. Natively unfolded proteins. Curr Opin Struct Biol. 2005; 15:35–41. [PubMed: 15718131]
3. Uversky VN, Gillespie JR, Fink AL. Why are “Natively Unfolded” Proteins Unstructured Under Physiologic Conditions? Proteins. 2000; 41:415–427. [PubMed: 11025552]
4. Uversky VN. Natively Unfolded Proteins: A Point Where Biology Waits for Physics. Protein Sci. 2002; 11:739–756. [PubMed: 11910019]

5. Iakoucheva LM, Radivojac P, Brown CJ, O'Connor TR, Sikes JG, Obradovic Z, Dunker AK. The Importance of Intrinsic Disorder for Protein Phosphorylation. Nucleic Acids Res. 2004; 32:1037–1049. [PubMed: 14960716]
6. Dunker AK, Obradovic Z. The Protein Trinity-Linking Function and Disorder. Nat Biotechnol. 2001; 19:805–806. [PubMed: 11533628]
7. Oldfield CJ, Cheng Y, Cortese MS, Romero P, Uversky VN, Dunker AK. Coupled folding and binding with alpha-helix-forming molecular recognition elements. Biochemistry. 2005; 44:12454–12470. [PubMed: 16156658]
8. Mohan A, Sullivan WJJ, Radivojac P, Dunker AK, Uversky VN. Intrinsic disorder in pathogenic and non-pathogenic microbes: discovering and analyzing the unfoldomes of early-branching eukaryoryotes. MolBiosyst. 2008; 4:328–340.
9. Vacic V, Oldfield CJ, Mohan A, Radivojac P, Cortese MS, Uversky VN, Dunker AK. Characterization of molecular recognition features, MoRFs, and their binding partners. J Proteome Res. 2007; 6:2351–2366. [PubMed: 17488107]
10. Dunker AK, Lawson JD, Brown CJ, Williams RM, Romero P, Oh JS, Oldfield CJ, Campen AM, Ratliff CM, Hipps KW, Ausio J, Nissen MS, Reeves R, Kang C, Kissinger CR, Bailey RW, Griswold MD, Chiu W, Garner EC, Obradovic Z. Intrinsically Disordered Protein. J Mol Graph Model. 2001; 19:26–59. [PubMed: 11381529]
11. Dunker AK, Brown CJ, Lawson JD, Iakoucheva LM, Obradovic Z. Intrinsic Disorder and Protein Function. Biochemistry. 2002; 41:6573–6582. [PubMed: 12022860]
12. Dunker AK, Brown CJ, Obradovic Z. Identification and functions of usefully disordered proteins. Adv Protein Chem. 2002; 62:25–49. [PubMed: 12418100]
13. Dunker AK, Cortese MS, Romero P, Iakoucheva LM, Uversky VN. Flexible nets. The roles of intrinsic disorder in protein interaction networks. FEBS J. 2005; 272:5129–5148. [PubMed: 16218947]
14. Wright PE, Dyson HJ. Intrinsically unstructured proteins: re-assessing the protein structure-function paradigm. J Mol Biol. 1999; 293:321–331. [PubMed: 10550212]
15. Dyson HJ, Wright PE. Intrinsically Unstructured Proteins and their Functions. Nat Rev Mol Cell Biol. 2005; 6:197–208. [PubMed: 15738986]
16. Daughdrill, GW.; Pielak, GJ.; Uversky, VN.; Cortese, MS.; Dunker, AK. Natively Disordered Proteins. In: Buchner, J.; Kiefhaber, T., editors. Handbook of Protein. 2005. p. 271-353.
17. Uversky VN, Oldfield CJ, Dunker AK. Showing Your ID: Intrinsic Disorder as an ID for Recognition, Regulation and Cell Signaling. J Mol Recognit. 2005; 18:343–384. [PubMed: 16094605]
18. Iakoucheva LM, Brown CJ, Lawson JD, Obradovic Z, Dunker AK. Intrinsic disorder in cell-signaling and cancer-associated proteins. J Mol Biol. 2002; 323:573–584. [PubMed: 12381310]
19. Oldfield CJ, Meng J, Yang JY, Yang MQ, Uversky VN, Dunker AK. Flexible nets: Disorder and induced fit in the associations of p53 and 14-3-3 with their partners. BMC Genomics. 2008; 9(Suppl 1):S1.
20. Uversky VN, Oldfield CJ, Dunker AK. Intrinsically disordered proteins in human diseases: Introducing the D2 concept. Ann Rev Biophys Biomol Structure. 2008; 37:215–246.
21. Dunker AK, Obradovic Z, Romero P, Garner EC, Brown CJ. Intrinsic protein disorder in complete genomes. Genome Inform Ser Workshop Genome Inform. 2000; 11:161–171.
22. Chen SW, Romero P, Uversky VN, Dunker AK. Conservation of protein disorder in protein domain and families I. A database of conserved predicted disordered regions. J Prot Res. 2006; 5:879–887.
23. Kriwacki RW, Hengst L, Tennant L, Reed SI, Wright PE. Structural studies of p21Waf1/Cip1/Sdi1 in the free and Cdk2-bound state: conformational disorder mediates binding diversity. Proc Natl Acad Sci U S A. 1996; 93:11504–11509. [PubMed: 8876165]
24. Schwob E, Bohm T, Mendenhall MD, Nasmyth K. The B-type cyclin kinase inhibitor p40SIC1 controls the G1 to S transition in S. cerevisiae. Cell 79. 1994; 1994:233–244.
25. Deshaies RJ, Ferrell JEJ. Multisite phosphorylation and the countdown to S phase. Cell. 2001; 107:819–822. [PubMed: 11779457]

26. Verma R, Annan RS, Huddleston MJ, Carr SA, Reynard G, Deshaies RJ. Phosphorylation of Sic1p by G1 Cdk required for its degradation and entry into S phase. Science. 1997; 278:455–460. [PubMed: 9334303]
27. Coccetti P, Rossi R, Sternieri F, Porro D, Russo GL, di Fonzo A, Magni F, Vanoni M, Alberghina L. Mutations of the CK2 phosphorylation site of Sic1 affect cell size and S-Cdk kinase activity in Saccharomyces cerevisiae. Mol Microbiol. 2004; 51:447–460. [PubMed: 14756785]
28. Coccetti P, Zinzalla V, Tedeschi G, Russo GL, Fantinato S, Marin O, Pinna LA, Vanoni M, Alberghina L. Sic1 is phosphorylated by CK2 on Ser201 in budding yeast cells. Biochem Biophys Res Commun. 2006; 346:786–793. [PubMed: 16777072]
29. Barberis M, Klipp E, Vanoni M, Alberghina L. Cell size at S phase initiation: an emergent property of the G1/S network. PLoS. 2007; 3:e64.
30. Rossi RL, Zinzalla V, Mastriani A, Vanoni M, Alberghina L. Subcellular localization of the cyclin dependent kinase inhibitor Sic1 is modulated by the carbon source in budding yeast. Cell Cycle. 2005; 4:1798–1807. [PubMed: 16294029]
31. Zinzalla V, Graziola M, Mastriani A, Vanoni M, Alberghina L. Rapamycin-mediated G1 arrest involves regulation of the Cdk inhibitor Sic1 in Saccharomyces cerevisiae. Mol Microbiol. 2007; 63:1482–1494. [PubMed: 17302822]
32. Escote X, Zapater M, Clotet J, Posas F. Hog1 mediates cell-cycle arrest in G1 phase by the dual targeting of Sic1. Nat Cell Biol. 2004; 6:997–1002. [PubMed: 15448699]
33. Hodge A, Mendenhall M. The cyclin-dependent kinase inhibitory domain of the yeast Sic1 protein is contained within the C-terminal 70 amino acids. Mol Gen Genet. 1999; 1:55–64. [PubMed: 10503536]
34. Barberis M, De Gioia L, Ruzzene M, Sarno S, Coccetti P, Fantucci P, Vanoni M, Alberghina L. The yeast cyclin-dependent kinase inhibitor Sic1 and mammalian p27Kip1 are functional homologues with a structurally conserved inhibitory domain. Biochem J. 2005; 387:639–647. [PubMed: 15649124]
35. Bowman P, Galea CA, Lacy E, Kriwacki RW. Thermodynamic characterization of interactions between p27(Kip1) and activated and non-activated Cdk2: intrinsically unstructured proteins as thermodynamictethers. Biochim Biophys Acta. 2006; 1764:182–189. [PubMed: 16458085]
36. Sivakolundu SG, Bashford D, Kriwacki RW. Disordered p27Kip1 exhibits intrinsic structure resembling the Cdk2/cyclin A-bound conformation. J Mol Biol. 2005; 353:1118–1128. [PubMed: 16214166]
37. Russo AA, Jeffrey PD, Patten AK, Massague J, Pavletich NP. Crystal structure of the p27Kip1 cyclin-dependent-kinase inhibitor bound to the cyclin A-Cdk2 complex. Nature. 1996; 382:325–331. [PubMed: 8684460]
38. Barberis M, Pagano MA, Gioia LD, Marin O, Vanoni M, Pinna LA, Alberghina L. CK2 regulates in vitro the activity of the yeast cyclin-dependent kinase inhibitor Sic1. Biochem Biophys Res Commun. 2005; 336:1040–1048. [PubMed: 16168390]
39. Tripodi F, Zinzalla V, Vanoni M, Alberghina L, Coccetti P. In CK2 inactivated cells the cyclin dependent kinase inhibitor Sic1 is involved in cell-cycle arrest before the onset of S phase. Biochem Biophys Res Commun. 2007; 359:921–927. [PubMed: 17574209]
40. Dyson HJ, Wright PE. Unfolded proteins and protein folding studied by NMR. Chem Rev. 2004; 104:3607–3622. [PubMed: 15303830]
41. Receveur-Brechot V, Bourhis JM, Uversky VN, Canard B, Longhi S. Assessing Protein Disorder and Induced Folding. Proteins. 2006; 62:24–45. [PubMed: 16287116]
42. Li X, Romero P, Rani M, Dunker AK, Obradovic Z. Predicting Protein Disorder for N-, C-, and Internal Regions. Genome Inform Ser Workshop Genome Inform. 1999; 10:30–40.
43. Peng K, Vucetic S, Radivojac P, Brown CJ, Dunker AK, Obradovic Z. Optimizing long intrinsic disorder predictors with protein evolutionary information. J Bioinform Comput Biol. 2005; 3:35–60. [PubMed: 15751111]
44. Romero P, Obradovic Z, Li X, Garner EC, Brown CJ, Dunker AK. Sequence complexity of disordered protein. Proteins. 2001; 42:38–48. [PubMed: 11093259]

45. Dosztanyi Z, Csizmok V, Tompa P, Simon I. IUPred: web server for the prediction of intrinsically unstructured regions of proteins based on estimated energy content. Bioinformatics. 2005; 21:3433–3434. [PubMed: 15955779]
46. Yang ZR, Thomson R, McNeil P, Esnouf RM. RONN: the bio-basis function neural network technique applied to the detection of natively disordered regions in proteins. Bioinformatics. 2005; 21:3369–3376. [PubMed: 15947016]
47. Cheng Y, Oldfield CJ, Meng J, Romero P, Uversky VN, Dunker AK. Mining alpha-helix-forming molecular recognition features with cross species sequence alignments. Biochem. 2007; 46:13468–13477. [PubMed: 17973494]
48. Obradovic Z, K. Peng K, Vucetic S, Radivojac P, C.J. B. Predicting intrinsic disorder from amino acid sequence. Proteins. 2003; 53:566–572. sequence. DAKPidfaa. [PubMed: 14579347]
49. Obradovic Z, Peng K, Vucetic S, Radivojac P, Dunker AK. Exploiting heterogeneous sequence properties improves prediction of protein disorder. Prot Struct Funct and Bioinformatics. 2005; 61:176–182.
50. Dosztányi Z, Csizmók V, Tompa P, Simon I. The pairwise energy content estimated from amino acid composition discriminates between folded and intrinsically unstructured proteins. J Mol Biol. 2005; 347:827–839. [PubMed: 15769473]
51. Oldfield CJ, Cheng Y, Cortese MS, Brown CJ, Uversky VN, Dunker AK. Comparing and combining predictors of mostly disordered proteins. Biochemistry. 2005; 44:1989–2000. [PubMed: 15697224]
52. Vacic V, Uversky VN, Dunker AK, Lonardi S. Composition Profiler: A tool for discovery and visualization of amino acid composition differences. BMC Bioinformatics. 2007; 8:211. [PubMed: 17578581]
53. Sickmeier M, Hamilton JA, LeGall T, Vacic V, Cortese MS, Tantos A, Szabo B, Tompa P, Chen J, Uversky VN, Obradovic Z, Dunker AK. DisProt: The database of disordered proteins. Nucleic Acids Res. 2007; 35:D786–793. [PubMed: 17145717]
54. Sambrook, J.; Fritsch, EF.; Maniatis, T. A laboratory manual. Cold Spring Harbor Laboratory Press; Cold Spring Harbor, NY: 1989. Molecular cloning.
55. Matsumura I, Rowe LA. Whole plasmid mutagenic PCR for directed protein evolution. Biomol Engineering. 2005; 22:73–79.
56. Laemmli UK. Cleavage of structural proteins during the assembly of the head of bacteriophage T4. Nature. 1970; 5259:680–685. [PubMed: 5432063]
57. Savitsky A, Golay MJE. Smoothing and differentiation of data by simplified least squares procedures. Anal Chem. 1964; 36:1627–1639.
58. Sreerama N, Woody RW. Estimation of protein secondary structure from circular dichroism spectra: comparison of CONTIN, SELCON, and CDSSTR methods with an expanded reference set. Anal Biochem. 2000; 287:252–260. [PubMed: 11112271]
59. Ouali M, King RD. Cascaded multiple classifiers for secondary structure prediction. Prot Sci. 2000; 9:1162–1176.
60. Linding R, Russell RB, Neduva V, T.J. G. GlobPlot: exploring protein sequences for globularity and disorder. Nucleic Acid Res. 2003; 31
61. Tompa P. Intrinsically unstructured proteins. Trends Biochem Sci. 2002; 27:527–533. [PubMed: 12368089]
62. Sobott F, McCammon MG, Hernandez H, Robinson CV. The flight of macromolecular complexes in a mass spectrometer. Philos Transact A Math Phys Eng Sci. 2005; 363:379–389. [PubMed: 15664889]
63. Ashcroft AE. Recent developments in electrospray ionisation mass spectrometry: noncovalently bound protein complexes. Nat Prod Rep. 2005; 22:452–464. [PubMed: 16047045]
64. Sharon M, Robinson CV. The Role of Mass Spectrometry in Structure Elucidation of Dynamic Protein Complexes. Ann Rev Biochem. 2007; 76:167–193. [PubMed: 17328674]
65. Uversky VN. What does it mean to be natively unfolded? Eur J Biochem. 2002; 269:2–12. [PubMed: 11784292]
66. Kaltashov IA, Abzalimov RR. Do ionic charges in ESI MS provide useful information on macromolecular structure? J Am Soc Mass Spectrom. 2008; 19:1239–1246. [PubMed: 18602274]

67. Konermann L. A minimalist model for exploring conformational effects on the electrospray charge state distribution of proteins. J Phys Chem B. 2007; 111:6534–6543. [PubMed: 17511498]
68. Smith DP, Giles K, Bateman RH, Radford SE, Ashcroft AE. Monitoring copopulated conformational states during protein folding events using electrospray ionization-ion mobility spectrometry-mass spectrometry. J Am Soc Mass Spectrom. 2007; 18:2180–2190. [PubMed: 17964800]
69. Borysik AJ, Radford SE, Ashcroft AE. Co-populated conformational ensembles of beta2-microglobulin uncovered quantitatively by electrospray ionization mass spectrometry. J Biol Chem. 2004; 279:27069–27077. [PubMed: 15100226]
70. Grandori R. Electrospray-ionization mass spectrometry for protein conformational studies. Curr Org Chem. 2003; 7:1589–1603.
71. Grandori R, Matecko I, Müller N. Uncoupled analysis of secondary and tertiary protein structure by circular dichroism and electrospray ionization mass spectrometry. J Mass Spectrom. 2001; 37:191–196. [PubMed: 11857763]
72. Bernstein SL, Liu D, Wyttenbach T, Bowers MT, Lee JC, Gray HB, Winkler JR. Alpha-synuclein: stable compact and extended monomeric structures and pH dependence of dimer formation. J Am Soc Mass Spectrom. 2004; 15:1435–1443. [PubMed: 15465356]
73. Yi S, Boys BL, Brickenden A, Konermann L, Choy WY. Effects of zinc binding on the structure and dynamics of the intrinsically disordered protein prothymosin alpha: evidence for metalation as an entropic switch. Biochemistry. 2007; 46:13120–13130. [PubMed: 17929838]
74. Heck AJ, Van Den Heuvel RH. Investigation of intact protein complexes by mass spectrometry. Mass Spectrom Rev. 2004; 23:368–389. [PubMed: 15264235]
75. Buck M. Trifluoroethanol and colleagues: cosolvents come of age. Recent studies with peptides and proteins. Q Rev Biophys. 1998; 31:297–355. [PubMed: 10384688]
76. Morin B, Bourhis JM, Belle V, Woudstra M, Carrière F, Guigliarelli B, Fournel A, Longhi S. Assessing induced folding of an intrinsically disordered protein by site-directed spin-labeling electron paramagnetic resonance spectroscopy. J Phys Chem B. 2006; 110:20596–20608. [PubMed: 17034249]
77. Fontana A, de Laureto PP, Spolaore B, Frare E, Picotti P, Zambonin M. Probing protein structure by limited proteolysis. Acta Biochim Pol. 2004; 51:299–321. [PubMed: 15218531]
78. Carey J. A systematic, general proteolytic method for defining structural and functional domains of proteins. Methods in Enzymol. 2000; 328:499–514. [PubMed: 11075363]
79. Hubbard SJ, Campbell SF, Thornton JM. Molecular recognition. Conformational analysis of limited proteolytic sites and serine proteinase protein inhibitors. J Mol Biol. 1991; 220:507–530. [PubMed: 1856871]
80. Fontana A, Fassina G, Vita C, Dalzoppo D, Zamai M, Zambonin M. Correlation between sites of limited proteolysis and segmental mobility in thermolysin. Biochemistry. 1986; 25:1847–1851. [PubMed: 3707915]
81. Novotny J, Bruccoleri RE. Correlation among sites of limited proteolysis, enzyme accessibility and segmental mobility. FEBS Lett. 1987; 211:185–189. [PubMed: 3542567]
82. Hubbard SJ, Beynon RJ, Thornton JM. Assessment of conformational parameters as predictors of limited proteolytic sites in native protein structures. Protein Eng. 1998; 11:349–359. [PubMed: 9681867]
83. Hubbard SJ, Eisenmenger F, Thornton JM. Modeling studies of the change in conformation required for cleavage of limited proteolytic sites. Protein Sci. 1994; 3:757–768. [PubMed: 7520312]
84. Fontana A, Polverino de Laureto P, De Filippis V, Scaramella E, Zambonin M. Probing the partly folded states of proteins by limited proteolysis. Fold Des. 1997; 2:R17–26. [PubMed: 9135978]
85. Iakoucheva LM, Kimzey AL, Masselon CD, Bruce JE, Garner EC, Brown CJ, Dunker AK, Smith RD, Ackerman EJ. Identification of intrinsic order and disorder in the DNA repair protein XPA. Protein Sci. 2001; 10:560–571. [PubMed: 11344324]
86. Longhi S, Receveur-Bréchot V, Karlin D, Johansson K, Darbon H, Bhella D, Yeo R, Finet S, Canard B. The C-terminal domain of the measles virus nucleoprotein is intrinsically disordered

and folds upon binding to the C-terminal moiety of the phosphoprotein. J Biol Chem. 2003; 278:18638–18648. [PubMed: 12621042]

87. Mark WY, Liao JC, Lu Y, Ayed A, Laister R, Szymczyna B, Chakrabartty A, Arrowsmith CH. Characterization of segments from the central region of BRCA1: an intrinsically disordered scaffold for multiple protein-protein and protein-DNA interactions? J Mol Biol. 2005; 345:275–287. [PubMed: 15571721]
88. de Laureto PP, Tosatto L, Frare E, Marin O, Uversky VN, Fontana A. Conformational properties of the SDS-bound state of alpha-synuclein probed by limited proteolysis: unexpected rigidity of the acidic C-terminal tail. Biochemistry. 2006; 45:11523–11531. [PubMed: 16981712]
89. Mittag T, Orlicky S, Choy WY, Tang X, Lin H, Sicheri F, Kay LE, Tyers M, Forman-Kay JD. Dynamic equilibrium engagement of a polyvalent ligand with a single-site receptor. PNAS. 2008; 105:17772–17777. [PubMed: 19008353]
90. Hua QX, Jia WH, Bullock BP, Habener JF, Weiss MA. Transcriptional activator-coactivator recognition: nascent folding of a kinase-inducible transactivation domain predicts its structure on coactivator binding. Biochemistry. 1998; 37:5858–5866. [PubMed: 9558319]
91. Wallon G, Rappsilber J, Mann M, Serrano L. Model for stathmin/OP18 binding to tubulin. EMBO J. 2000; 19:213–222. [PubMed: 10637225]
92. Zitzewitz JA, Ibarra-Molero B, Fishel DR, Terry KL, Matthews CR. Preformed secondary structure drives the association reaction of GCN4-p1, a model coiled-coil system. J Mol Biol. 2000; 296:1105–1116. [PubMed: 10686107]
93. Wang Y, Filippov I, Richter C, Luo R, Kriwacki RW. Solution NMR studies of an intrinsically unstructured protein within a dilute, 75 kDa eukaryotic protein assembly; probing the practical limits for efficiently assigning polypeptide backbone resonances. ChemBioChem. 2005; 6:2242–2246. [PubMed: 16270364]
94. Lacy ER, Filippov I, Lewis WS, Otieno S, Xiao L, Weiss S, Hengst L, Kriwacki RW. p27 binds cyclin-CDK complexes through a sequential mechanism involving binding-induced protein folding. Nat Struct Mol Biol. 2004; 11:358–364. [PubMed: 15024385]
95. Galea CA, Nourse A, Wang Y, Sivakolundu SG, Heller WT, Kriwacki RW. Role of intrinsic flexibility i signal transduction mediated by the cell cycle regulator p27Kip1. J Mol Biol. 2008; 3:827–838. [PubMed: 18177895]
96. Lacy ER, Wang Y, Post J, Nourse A, Webb W, Mapelli M, Musacchio A, Siuzdak G, Kriwacki RW. Molecular basis for the specificity of p27 toward cyclin-dependent kinases that regulate cell division. J Mol Biol. 2005; 349:764–773. [PubMed: 15890360]
97. Tapia JC, Bolanos-Garcia VM, Sayed M, Allende CC, Allende JE. Cell cycle regulatory protein p27KIP1 is a substrate and interacts with the protein kinase CK2. J Cell Biochem. 2004; 91:865–879. [PubMed: 15034923]
98. Settimo L, Donnini S, Juffer AH, Woody RW, Marin O. Conformational changes upon calcium binding and phosphorylation in a synthetic fragment of calmodulin. Biopolymers. 2007; 88:373–385. [PubMed: 17173306]
99. Collins MO, Yu L, Campuzano I, Grant SGN, Choudary JS. Phosphoproteomic analysis of the mouse brain cytosol reveals a predominance of protein phoshorylation in regions of intrinsic sequence disorder. Mol Cell Proteomics. 2008; 7:1331–1348. [PubMed: 18388127]
100. Tarassov K, Messier V, Landry CR, Radinovic S, Molina MM, Shames I, Malitskaya Y, Vogel J, Bussey H, Michnick SW. An in vivo map of the yeast protein interactome. Science. 2008; 320:1465–1470. [PubMed: 18467557]
101. Klein P, Pawson T, Tyers M. Mathematical modeling suggests cooperative interactions between a disordered polyvalent ligand and a single receptor site. Curr Biol. 2003; 13:1669–1678. [PubMed: 14521832]
102. Tompa P, Fuxreiter M. Fuzzy complexes: polymorphism and structural disorder in protein-protein interaction. Trends Biochem Sci. 2008; 33:2–8. [PubMed: 18054235]
103. Borg M, Mittag T, Pawson T, Tyers M, Forman-Kay JD, Chan HS. Polyelectrostatic interactions of disordered ligands suggest a physical basis for ultrasensitivity. PNAS. 2007; 104:9650–9655. [PubMed: 17522259]

104. Vihinen M. Relationship of protein flexibility to thermostability. Protein Eng. 1987; 1:477–480. [PubMed: 3508295]

Figure 1.

Sic1 sequence analysis. Amino acid sequence and predicted structural features. *Jnet*, consensus secondary structure by *JPRED* (H, helix; E, extended); *SUBacc*, high confidence accessibility prediction by *PROFACC* (e, exposed; b, buried); *alpha MORF*, α-helical intermolecular recognition sites predicted by α-*MORF*; *Dock_model*, helical region predicted by the homology model of the inhibitory domain (residues 215-284).

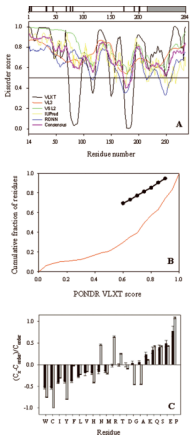

Figure 2.

Sic1 disorder propensity. A) Intrinsic-disorder predictions. The plot represents prediction results by *IUPred* (yellow line); *RONN* (blue line); *PONDR®VLXT* (black line), *PONDR®VL3* (red line), and *PONDR®VSL2* (green line). The average of these five predictions is shown as a bold pink line. At the top of the panel, schematic representation of the Sic1 molecule with indication of the known phosphorylation sites (black bars) and of the inhibitory domain (shaded box). B) CDF analysis. Data for Sic1 are shown by a red line. The thick black line with black circles represents the empirical boundary separating mostly ordered from mostly disordered proteins.53 C) Compositional profiling of Sic1. The plot shows the fractional difference in amino acid composition of Sic1 (gray bars) and of a set of intrinsically disordered proteins from the *DisProt* database104 (black bars) relative to a reference set of ordered, globular proteins. The fractional difference is calculated as $(C_X-C_{order})/C_{order}$, where C_X is the content in a given amino acid of Sic1 (or of the set of intrinsically disordered proteins) and C_{order} is the corresponding value in the set of ordered proteins. Negative fractional difference indicates depletion (and positive, enrichment) in the corresponding amino acid. Amino acids are arranged on the *x* axis from the most rigid to the most flexible according to the Vihinen's flexibility scale. Methionine at the N terminus and His-tags were not included in the calculation. The error bars correspond to the confidence intervals evaluated by the 10,000 bootstrap iterations in the definition of the reference protein sets.

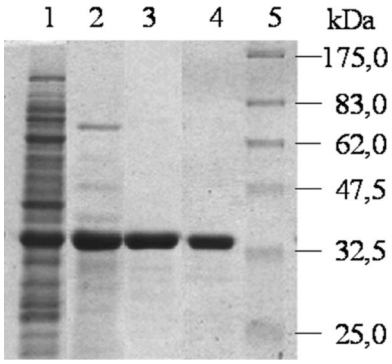

Figure 3.

Sic1 expression and purification. Coomassie-stained SDS-PAGE. Lane 1, crude extract; lane 2, supernatant of the heat-treated crude extract; lane 3, pooled fractions eluted from the IMAC column; lane 4, pooled fractions eluted from the PD10 column; lane 5, molecular-weight markers.

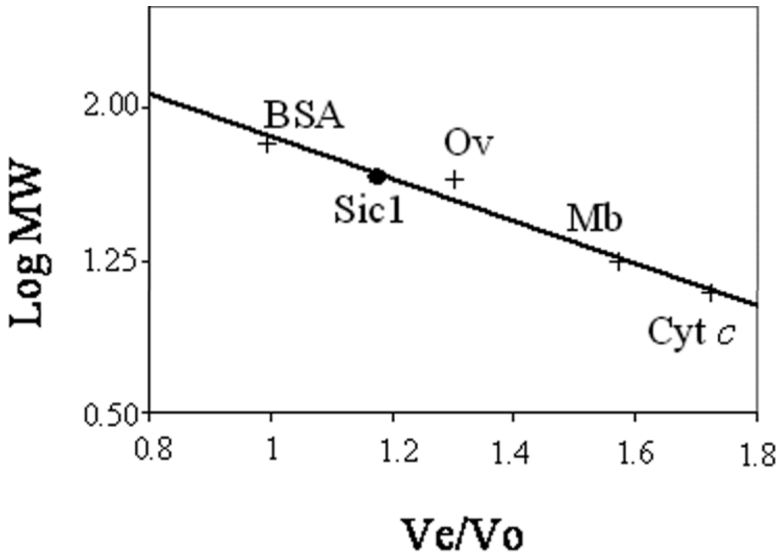

Figure 4.

Sic1 apparent molecular weight by gel filtration. The retention time of 10 μM pure Sic1 on a *Superdex-75* gel-filtration column in 50 mM sodium phosphate, pH 8.0, 200 mM NaCl is compared to that of globular proteins of known molecular weight (BSA, bovine serum albumin; Ov, ovalbumin; Mb, myoglobin; Cyt *c*, cytochrome *c*). Ve, elution volume; Vo, void volume. The derived apparent molecular weight of Sic1 is ~50 kDa.

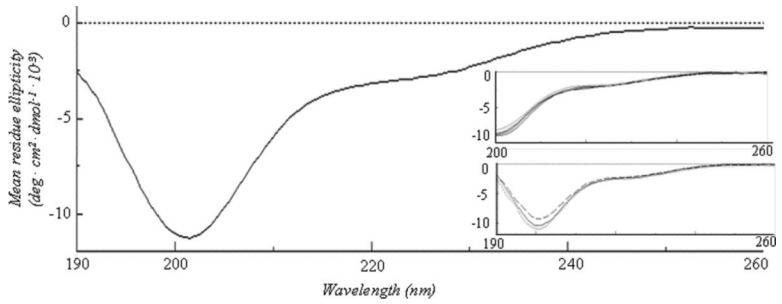

Figure 5.

Sic1 secondary structure by far-UV CD. Spectra of 5 μM Sic 1 in 50 mM sodium phosphate, pH 6.5. The upper inset shows the spectra at different NaCl concentrations: 0 (dotted) and 100, 200, 300 mM (solid). The lower inset shows the spectra of the mutants S201A (dotted) and S201E (dashed) compared to the wild-type protein (solid) in 50 mM sodium phosphate, pH 6.5.

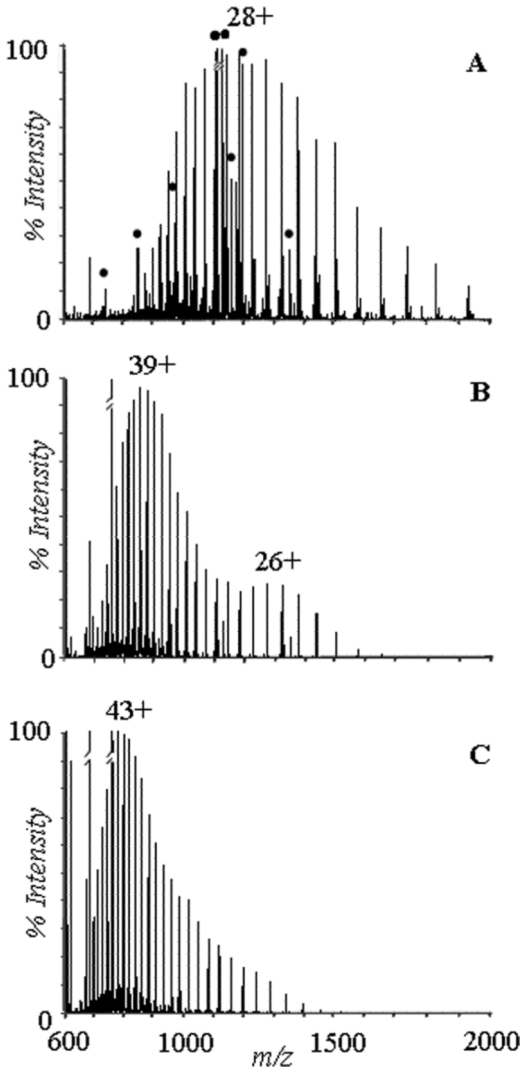

Figure 6.

Sic1 tertiary structure by nano-ESI-MS. Spectra of 15 μM intact Sic1 in A) 50 mM ammonium acetate, pH 6.5; B) 1% formic acid; C) 1% formic acid and 50% acetonitrile. Labels show the main charge state of each peak envelope. Peaks corresponding to Sic1 degradation products are marked by dots in the upper panel.

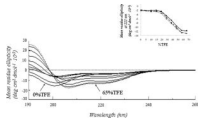

Figure 7.

Effect of TFE on Sic1 secondary structure by far-UV CD. Spectra of 5 μM Sic 1 in 50 mM sodium phosphate, pH 6.5 and increasing concentrations of TFE (0, 5, 10, 15, 20, 30, 40, 50, 60, 65%). The spectrum at 65% TFE is shown by a dotted line. The inset shows the plot of the mean residue ellipticity at 222 nm of the wild-type (solid), S201A (dotted) and S201E (dashed) proteins.

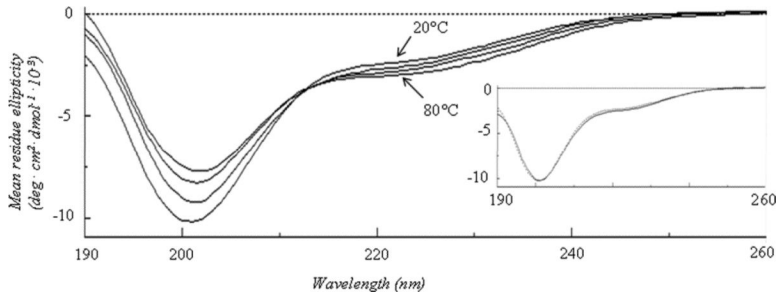

Figure 8.

Effect of heat on Sic1 secondary structure by far-UV CD. Spectra of 5 μM Sic1 in 50 mM sodium phosphate, pH 6.5, at 20, 40, 60 and 80 °C. The inset shows the Sic 1 spectrum before heat treatment (solid line) and after heat treatment and re-cooling at room temperature (dotted line).

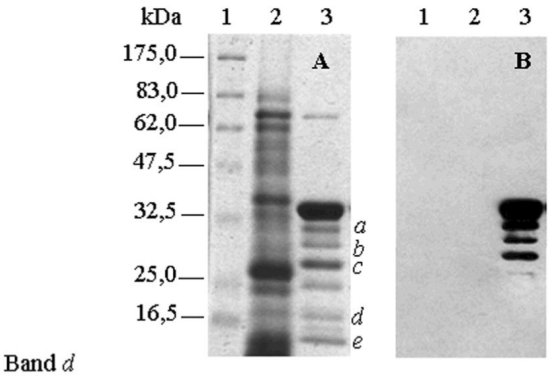

Band *d*

```
  1  MTPSTPPRSR GTRYLAQPSG NTSSSALMQG QKTPQKPSQN LVPVTPSTTK
 51  SFKNAPLLAP PNSNMGMTSP FNGLTSPQRS PFPKSSVKRT LFQFESHDNG
101  TVREEQEPLG RVNRILFPTQ QNVDIDAAEE EEEGEVLLPP SRPTSARQLH
151  LSLERDEFDQ THRKKIIKDV PGTPSDKVIT FELAKNWNNN SPKNDARSQE
201  SEDEEDIIIN PVRVGKNPFA SDELVTQEIR NERKRAMLRE NPDIEDVITY
251  VNKKGEVVEK RRLTDEEKRR FKPKALFQSR DQEHHHHHHH
```

Band *e*

```
  1  MTPSTPPRSR GTRYLAQPSG NTSSSALMQG QKTPQKPSQN LVPVTPSTTK
 51  SFKNAPLLAP PNSNMGMTSP FNGLTSPQRS PFPKSSVKRT LFQFESHDNG
101  TVREEQEPLG RVNRILFPTQ QNVDIDAAEE EEEGEVLLPP SRPTSARQLH
151  LSLERDEFDQ THRKKIIKDV PGTPSDKVIT FELAKNWNNN SPKNDARSQE
201  SEDEEDIIIN PVRVGKNPFA SDELVTQEIR NERKRAMLRE NPDIEDVITY
251  VNKKGEVVEK RRLTDEEKRR FKPKALFQSR DQEHHHHHHH
```

Figure 9.

Sic1 fragmentation. A) SDS PAGE, Coomassie stained. Lane 1, molecular-weight markers; lane 2, crude extract of a ΔSic1 strain; lane 3, Sic1 purified after 4-h IPTG induction. B) Western blot immunodecorated by polyclonal anti-His_6 antibodies (lanes as in A). The results of MS/MS analysis of Sic1 fragments are reported below the gels. Sequence stretches corresponding to fragments identified in each band are shown in black and underlined.

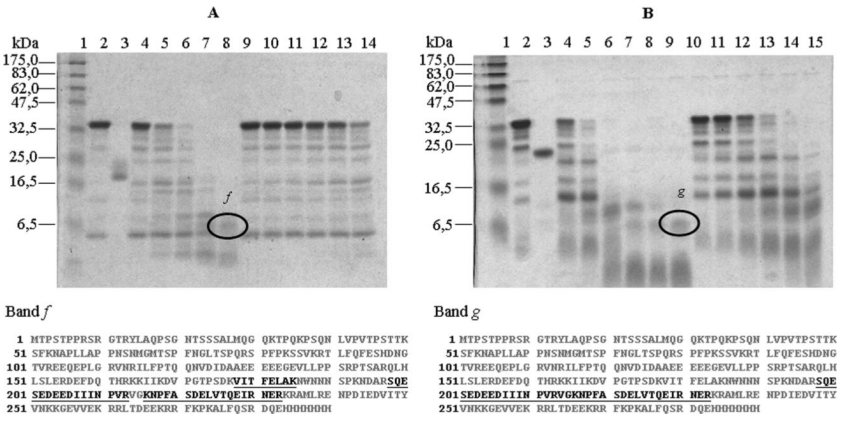

Figure 10.

Time course of Sic1 limited proteolysis by trypsin (A) and chymotrypsin (B) in 50 mM ammonium acetate, pH 6.5, 100 mM NaCl. Panel A: lane 1, molecular-weight markers; lane 2, starting Sic1 sample; lane 3, 1 μg trypsin; lanes 4-8 samples after 2, 5, 10, 15, 20 min digestion at 1:2000 enzyme:substrate (w/w ratio); lanes 9-14 samples after 1, 2, 5, 10, 15, 20 min digestion at 1:5000 enzyme:substrate (w/w ratio). Panel B: lane 1, molecular-weight markers; lane 2, starting Sic1 sample; lane 3, 1 μg chymotrypsin; lanes 4-9 samples after 1, 2, 5, 10, 15, 20 min digestion at 1:180 enzyme:substrate (w/w ratio); lanes 10-15 samples after 1, 2, 5, 10, 15, 20 min digestion at 1:900 enzyme:substrate ratio. The results of MS/MS analysis of Sic1 fragments are reported below the gels. Sequence stretches corresponding to fragments identified in each band are shown in black and underlined.